Geotechnical Aspects of Underground Construction in Soft Ground, Mair & Taylor (eds)
 ISBN 90 5410 856 8

Twin tunnel construction – Ground movements and lining behaviour

T.I. Addenbrooke & D.M. Potts
Imperial College of Science, Technology and Medicine, London, UK

ABSTRACT: The numerical analysis of twin tunnel construction has shown the shortcomings in the design assumption of superposition for both side by side and piggy back tunnel geometries. The interaction between two tunnels passing at depth has been shown to depend on relative tunnel position and spacing.

1 INTRODUCTION

Modern metro construction in congested urban environments often involves the excavation of new tunnels in close proximity to each other. In addition improvements to an existing network often requires new construction adjacent to existing tunnels. At the design stage it is therefore important to address the interaction of the tunnels and their effects on overall ground response. Unfortunately current design practice, which is based on empirical methods and rules of thumb, gives little guidance in this respect.

The ground surface settlement above multiple tunnel construction is commonly obtained by the superposition of individual settlement troughs obtained from empirical Gaussian distribution design curves for each tunnel in the geometry (New and O'Reilly, 1992). This implicitly assumes that the presence of an existing tunnel does not alter the expected ground movements into a new tunnel, and also does not account for any consolidation movement occurring when no engineering activity is taking place between construction of each tunnel.

The distortion to an existing tunnel lining induced by adjacent new tunnelling may be significant. Such considerations are not addressed by empirical design, and can only be assessed by numerical methods such as the finite element method.

A numerical parametric study has been undertaken to investigate twin tunnel behaviour. Two distinctly different geometries are considered, one with the tunnels running side by side at the same horizontal axis depth, and the other with the tunnels running one above the other, piggy back fashion, along the same vertical axis line. The spacing between the two tunnels is varied. The responses of both the ground surface, and the tunnel linings are considered. The validity of the assumption of superposition is addressed, and the differences in tunnel lining response are highlighted.

2 ANALYSIS DETAILS

2.1 Geometry and sequence of excavation.

The finite element code ICFEP (Imperial College Finite Element Program) was used to carry out ten separate analyses. In seven cases the excavation of two 4.146 m diameter running tunnels in London Clay was modelled, with a 22 day rest period between excavation of the first and the second. The side by side tunnels were all modelled at a depth of 34 m below ground level with centre line to centre line spacings of 8 ,12, 16, and 32 m. The lower tunnel of the piggy back tunnels was constant at 34 m below ground level, with upper tunnel axis levels of 24, 20, and 16 m below ground level, resulting in centre to centre spacings of 10, 14, and 18 m respectively. The lower tunnel was excavated first in each instance. Two tunnels excavated in close proximity with a rest period of 22 days are likely to be part of a single programme of works, and commonly the lower tunnel would be excavated first. Indeed this is the case with the Jubilee Line Extension work outside the Institution of Civil

Engineers where two tunnels were driven in piggy back fashion within a few months of each other, the lower tunnel being constructed first. Three further analyses were carried out to model single tunnel construction at axis depths of 24, 20, and 16 m below ground level, to provide comparisons with the twin tunnel piggy back results. For comparison with the ground surface response to the second of the side by side tunnels, the excavation of the first tunnel provided the greenfield single tunnel behaviour.

Figure 1 shows the relevant geometries and soil profile modelled. The pillar width and pillar depth (for side by side and piggy back respectively) are defined as the extrados to extrados dimension, that is the spacing less 2 tunnel radii.

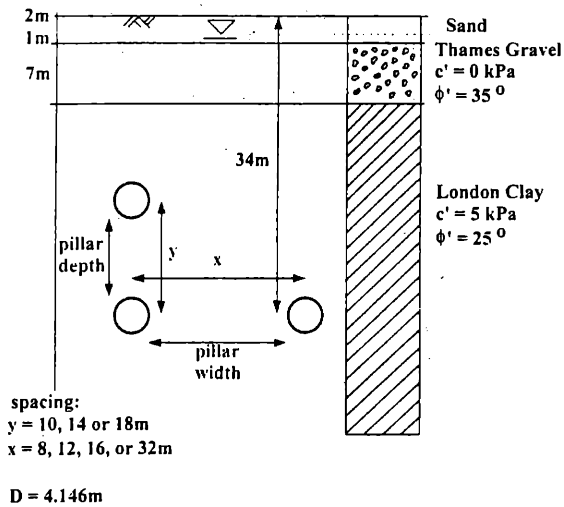

Figure 1. Twin tunnel geometry.

2.2 Finite element analysis.

The sand stratum at the surface was modelled as being linear elastic with a modulus of 5000 kPa. In the pre yield region, the Thames Gravel and the London Clay were both modelled with non linear elastic behaviour using a constitutive model of the form described by Jardine et al (1986); the model and parameters are detailed in Appendix A.

The Thames Gravel and London Clay were attributed the strength parameters shown in Figure 1. Plastic flow was defined by an angle of dilation equal to half the angle of shearing resistance, ϕ.

The sand and gravel were modelled as non consolidating materials whilst the London Clay was attributed with a linear isotropic permeability of 1×10^{-10} m/s.

The initial stresses prescribed a hydrostatic pore water pressure profile from a water table located 2 m below the ground surface, and a Coefficient of Earth Pressure at Rest, K_o of 0.5 in the sand and gravel, and 1.5 in the London Clay. All the soils had a bulk unit weight of 20 kN/m^3.

Coupled consolidation analysis was employed to model the construction of the tunnels and the rest periods. The soil was modelled by 8 noded isoparametric quadrilateral elements. The tunnel linings were modelled by 3 noded Mindlin beam elements (Day and Potts, 1990).

Excavation was modelled by removal of the solid elements within the circular tunnel boundary over a simulated time period of 8 hours. That is the stresses that the soil within the tunnel applied to the tunnel boundary were evaluated and then applied in the reverse direction over several increments. During this procedure the soil elements within the tunnel were not included in the analysis. The volume loss into the first tunnel was prescribed to be 1.4%. Volume loss was monitored against incremental progress and when the prescribed value was achieved the beam elements representing the tunnel lining were constructed. The beam elements modelled a 168 cm thick concrete lining, with a unit weight of 24 kN/m^3. The Young's Modulus was 28 x 10^6 kN/m^2, and the Poisson's Ratio was 0.15. As the excavation continued the remaining ground stresses were transferred into the tunnel lining resulting in stresses and bending moments existing on completion of excavation. A number of time increments were then modelled to represent the rest period. The excavation of the second tunnel followed the same pattern as the first, with the tunnel lining being constructed at the same relative increment of unloading. For the second excavation percentage unloading was therefore the controlled parameter, rather than the volume loss.

3 RESULTS

3.1 Surface settlement.

Side by side; in Figure 2 the shape of the short term surface settlement profile in response to the second tunnel excavation alone is plotted. The settlement, S, is normalised by the maximum settlement, S_{max}, and is plotted against the distance from the centre line of the tunnel being excavated. A numerically predicted greenfield settlement profile, which represents a no interaction situation is also plotted for direct comparison. It is evident that the shape of the settlement troughs above each of the second tunnels is very similar to the greenfield profile, but the lateral position of the maximum settlement is offset with respect to the tunnel centre line, towards the existing tunnel. The assumption of superposition would attribute a greenfield settlement profile to the second tunnel excavation, centred on the tunnel axis. The magnitude of S_{max} depends upon the volume loss into the second excavation. The reduced stiffness of the ground in the region of the second excavation influences the volume loss. For example, S_{max} above the second tunnel excavation located at a spacing of 8m from the first was 5.6mm, whilst for a spacing of 16m, S_{max} above the second tunnel was 5.05mm.

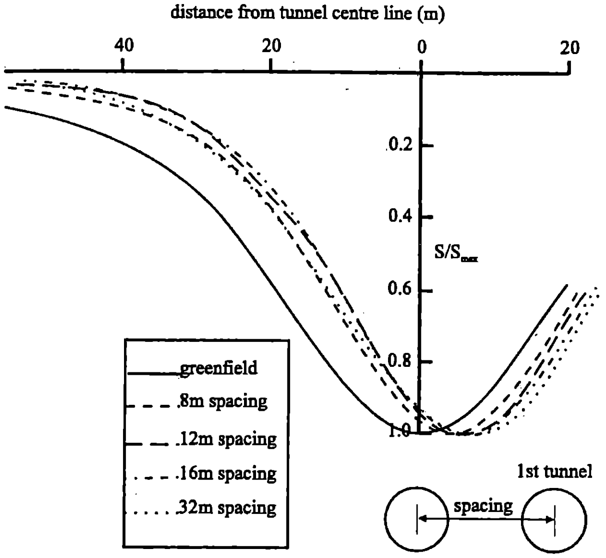

Figure 2. Settlement above 2nd of two side by side excavations.

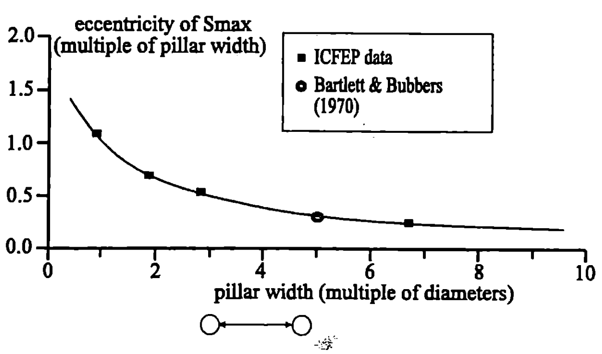

Figure 3. Eccentricity of S_{max} varying with pillar width (side by side tunnels).

Figure 3 shows how, for the settlement profile forming above the second excavation, the distance of the position of maximum settlement with respect to the tunnel centre line (the eccentricity of S_{max}) varies with pillar width. In the instance of zero interaction, the eccentricity is 0.0. A single available field data point is plotted for comparison. It is based on Bartlett and Bubbers (1970) interpretation of settlement measurements above a side by side, twin tunnel excavation which formed part of the Victoria Line construction. The data point lies on the trend indicated by the numerical study. With a pillar width less than 1 diameter, the eccentricity of S_{max} is tending toward a value equal to double the pillar width. The eccentricity (as a multiple of pillar width) reduces with increased spacing, down to less than 0.25 for a pillar width greater than 7 diameters.

Piggy back; Figure 4 compares the shape of the short term surface settlement profile as a result of the upper, second excavation with the numerically predicted greenfield settlement for a tunnel at the same axis depth. The settlement, S, has been normalised by the maximum settlement, S_{max}. For each depth of tunnel, the distance from the tunnel centre line, X, has been normalised by the trough width parameter for a greenfield profile above a tunnel of the same depth, i_g. The trough width parameter, i_g, is the distance from the tunnel centre line to the point of inflection of the settlement profile. This form of normalised plot results in the coincidence of the numerical greenfield profiles for all three depths of tunnel.

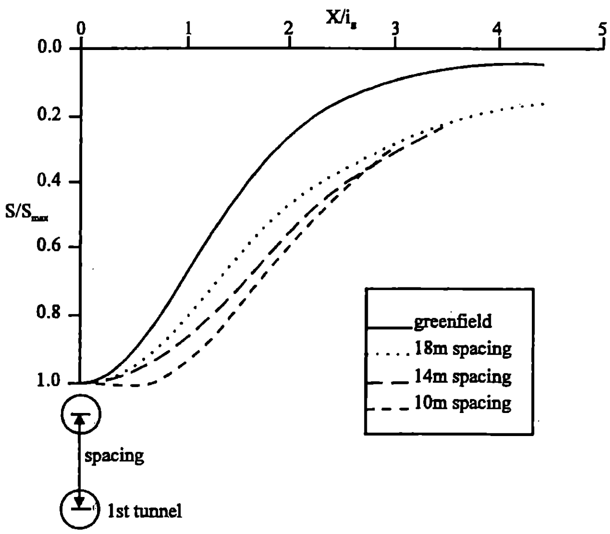

Figure 4. Settlement above the 2nd of two piggy back excavations.

All three comparisons (10 m, 14 m, and 18 m spacings) show the twin tunnel settlement to be wider than the greenfield profile. The shape of the settlement profile above the second tunnel excavation is different to the greenfield profile. The closer the spacing, the more flat bottomed the profile becomes above the tunnel centre line. The magnitude of S_{max} is dependent on the depth of the tunnel and the volume loss, which is influenced by the soils reduced stiffness in the zone of the second excavation.

In Figure 5 the distance from the tunnel centre line to the point of inflection of the settlement profiles above the second tunnel excavations, i, is plotted as a ratio to the greenfield i_g value, against the pillar depth. In the instance of zero interaction, i/i_g equals 1.0.

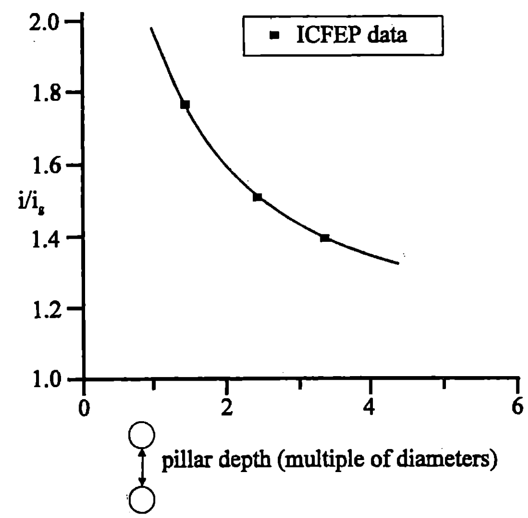

Figure 5. Position of inflection point varying with pillar depth (piggy back tunnels).

The trend shows an increase in trough width as the spacing reduces. For a pillar depth of less than 1 tunnel diameter, the profile can be twice as wide as the greenfield profile which would be assumed in superposition.

3.2 Tunnel lining response.

Figure 6 considers the influence of the excavation of the second tunnel on the lining to the first. For two side by side tunnels the existing tunnel lining is forced to squat on driving of the second tunnel. The horizontal diameter increases in length, whilst the vertical diameter reduces in length. For two piggy back tunnels the lining to the first tunnel elongates vertically on driving of the second tunnel. That is a lengthening of the vertical diameter, and a shortening of the horizontal diameter. Figure 6 shows how the magnitude of these two distortions vary with pillar width and depth:

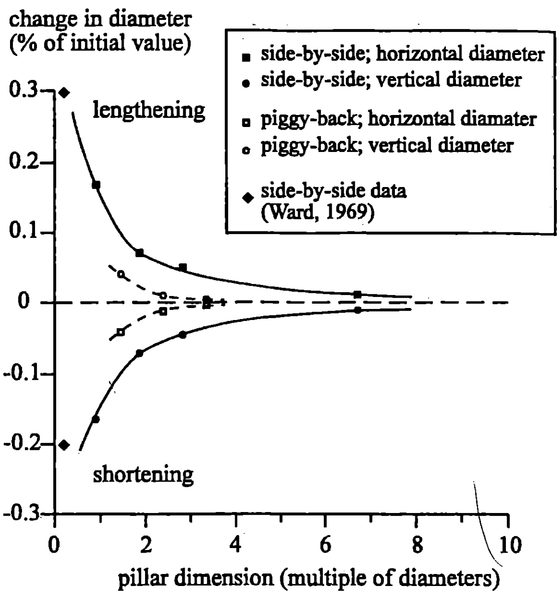

Figure 6. Response of 1st lining to passage of 2nd tunnel. (0.1% change in diameter is equal to 4mm over 4m.)

Side by side; when the pillar width is less than 1 diameter, the lengthening of the horizontal diameter is just under 0.2% of the initial diameter. This lengthening reduces with increased tunnel spacing. The shortening of the vertical diameter is also just under 0.2% of the initial diameter for the minimum pillar width analysed. The shortening of the vertical diameter reduces as spacing increases. Included on Figure 6 is data from the construction of the London Underground Victoria Line where two side by side tunnels were driven very close to one another (pillar width equal to 0.2 diameters) and the diametric variations in the first lining were recorded. The data points plotted here are the average of three very similar recordings reported by Ward (1969). Squatting distortions were recorded at all three locations, plotted as a lengthening of the horizontal diameter, and a shortening of the vertical diameter. The rest period was 35 days. The data lie outside the extent of the numerical analyses, but close to extrapolated trend lines indicated by the numerical data. The shortening of the vertical diameter is slightly less than that indicated by the numerical trend.

The implication is that with a pillar width of greater than 7 diameters the passage of a second tunnel at the same axis level as the existing tunnel could be considered not to distort or influence the existing tunnel lining constructed a few weeks previously.

Piggy back; none of the analyses exhibited a diametric distortion greater than 0.04% of the initial diameter. The lengthening of the vertical diameter (0.04% for a pillar width of just over 1 diameter) reduces as spacing increases. The shortening of the horizontal diameter (equal in magnitude to the vertical lengthening) also reduces as spacing increases.

In this case, the implication is that with a pillar depth greater than 3 diameters the passage of a second tunnel directly above the existing tunnel could be considered not to distort or influence the existing tunnel lining constructed a few weeks previously.

4 CONCLUSIONS

This paper has shown the influence of tunnel position on the interaction between two tunnels constructed within a month of each other. The ground surface response is dependent on whether the two tunnels are side by side, or one above the other. The spacing of the two tunnels also has a bearing on the ground surface response for both geometries. The influence that the driving of a second tunnel has on the lining previously installed in the first tunnel also depends upon relative tunnel position (to the side or vertically above) and on the spacing. Driving a new tunnel above an existing tunnel has significantly less influence on the existing tunnel lining than driving a new tunnel to the side.

4.1 Side by side.

- The assumption of superposition fails to account for the offset of the settlement profile from the centre line of the second tunnel excavation which was evident from the numerical results (Figure 2).
- The position of the maximum settlement above the second excavation can be estimated from Figure 3, which relates the eccentricity of S_{max} to pillar width. This curve may be dependent on tunnel depth, as all the numerical analyses modelled 34m deep tunnels. However, Bartlett and Bubbers (1970) data point fits the trend line, and is for two tunnels 21m below ground level.
- The horizontal diameter of the first tunnel lengthens, and the vertical diameter shortens on passage of the second tunnel. The magnitude of this induced squatting distortion reduces with increasing tunnel spacing, and is negligible for pillar widths greater than 7 tunnel diameters (Figure 6).

4.2 Piggy back.

- The assumption of superposition does not recognise the wider, flatter shape of settlement profile forming above the second, shallower tunnel excavation which was evident from the numerical results (Figure 4). The settlement above the second excavation is not of a Gaussian form, as assumed for greenfield situations.
- The distance to the point of inflection of the settlement profile as a result of interaction has been shown in Figure 5 to depend on the tunnel spacing.
- The horizontal diameter of the first tunnel shortens, and the vertical diameter lengthens on passage of the second tunnel. The magnitude of this induced elongated distortion reduces with increasing tunnel spacing, and is negligible for pillar depths greater than 3 tunnel diameters (Figure 6).

5 ACKNOWLEDGEMENTS

The work presented here has been sponsored by London Underground Limited as part of a wider research project into subsidence due to tunnelling and its interaction with buildings.

6 REFERENCES

Bartlett, J. V. & Bubbers, B. L. (1970). Surface movements caused by bored tunnelling. *Conference on subway construction*, Budapest - Balatonfured, pp 513 - 539.

Day, R. A. & Potts, D. M. (1990). Curved Mindlin beam and axi-symmetric shell elements - a new approach, *Int. Jnl. Num. Meth. Eng.*, Vol 30, pp 1263 - 1274.

Jardine, R. J., Potts, D. M., Fourie, A. B. & Burland, J. B. (1986). Studies of the influence of nonlinear stress-strain characteristics in soil-structure interaction, *Geotechnique*, Vol. 36, No. 3, pp 377 - 396.

New, B. M. & O'Reilly, M. P. (1991). Tunnelling induced ground movements; predicting their magnitude and effects, *Proc. of the 4th Int. Conf. on Ground Movements and Structures*, Cardiff, Ed. Geddes, pp 671 - 697.

O'Reilly, M. P. & New, B. M. (1982). Settlements above tunnels in the United Kingdom - their magnitude and prediction, *Tunnelling '82*, The Instn. of Mining and Metallurgy, pp 173 - 181.

Ward, W. H. (1969). Deep excavations and tunnelling in soft ground - discussion of paper by Peck, R. B.. *Proc. of the 7th Int. Conf. on Soil Mech. and Found. Engng.*, Mexico City, Vol. 3, pp 320 - 325.

APPENDIX A

Small strain non linear stiffness.

The secant stiffness expressions that describe the variation of shear and bulk moduli are:

$$\frac{3G}{p'} = A + B\cos\left[\alpha\left(\log_{10}\left(\frac{E}{\sqrt{3}C}\right)\right)^{\gamma}\right]$$

$$\frac{K}{p'} = R + S\cos\left[\delta\left(\log_{10}\frac{(\epsilon_v)}{T}\right)^{\lambda}\right]$$

where, G is the secant shear modulus, K is the secant bulk modulus, p' is the mean effective stress, E is the strain invariant used in ICFEP, and is related to ε_a (the axial strain observed in undrained triaxial tests) by the expression:

$$E = \sqrt{3}\,\epsilon_a$$

where,

$$E = 2\sqrt{\frac{1}{6}\left((\epsilon_1-\epsilon_2)^2 + (\epsilon_1-\epsilon_3)^2 + (\epsilon_2-\epsilon_3)^2\right.}$$

ε_1, ε_2, and ε_3 are principal strains, ε_v is the volumetric strain, and A, B, C, R, S, T, δ, α, γ and λ are all constants. Throughout the analyses the stiffness at a particular point is continually changing. It depends on both the current strain and the current mean effective stress at that point. Until a specified minimum strain, E_{min} is exceeded the shear stiffness varies only with the mean effective stress. This condition also applies once a specified upper strain limit is exceeded, E_{max}. Likewise, until a specified minimum volumetric strain, ε_{vmin} is exceeded the bulk stiffness varies only with the mean effective stress, and this condition applies once a specified upper strain limit, ε_{vmax} is exceeded. In the analyses the magnitude of the stiffness is prevented from falling below specified minimum values (G_{min} or K_{min}).

Coefficients and Limits for Non-Linear Shear and Bulk Modulus Expressions:

Strata	Thames Gravel	London Clay
A	1380.0	1120.0
B	1248.0	1016.0
C (%)	5.0×10^{-4}	1.0×10^{-4}
α	0.974	1.335
γ	0.940	0.617
E_{min} (%)	8.83346×10^{-4}	8.66025×10^{-4}
E_{max} (%)	0.34641	0.692820
G_{min} (kPa)	2000.0	2333.3
R	275.0	549.0
S	225.0	506.0
T	2.0×10^{-3}	1.0×10^{-3}
δ	0.998	2.069
λ	1.044	0.420
$\varepsilon_{v\,min}$ (%)	2.1×10^{-3}	5.0×10^{-3}
$\varepsilon_{v\,max}$ (%)	0.20	0.15
K_{min} (kPa)	5000.0	3000.0